

Entropic effects in carbon nanotubes-templated crystallization of Poly(3-alkyl thiophenes, P3HT, P3OT)



Yoav Dias, Rachel Yerushalmi-Rozen*

Department of Chemical Engineering, and The Ilse Katz Institute for Nanoscale Science and Technology, Beer-Sheva, Israel

ARTICLE INFO

Article history:

Received 5 August 2013

Received in revised form

25 September 2013

Accepted 28 September 2013

Available online 4 October 2013

Keywords:

Polymer crystallization

Entropic nucleation

Carbon nanotubes

ABSTRACT

A significant increase in polymer crystallinity is reported in composites of carbon-nanotubes (CNT) and Poly(3-octylthiophene-2,5-diyl), P3HT and Poly(3-octylthiophene-2,5-diyl), P3OT; Differential scanning calorimetry (DSC) reveal an increase from about 40% crystallinity of the native P3HT to ~62% in composites containing 25 wt% MWNT. A similar behavior is observed in P3OT with ~68% crystallinity, a double crystallization peak and higher melting temperature than the native polymers. The effect is unique to CNT and is not induced by fullerenes or graphene layers. High-resolution transmission electron microscopy, (HRTEM) of CNT-polymer dispersions reveal chains stacked upon the CNT in an elongated, stretched conformation. Following a detailed molecular study by Bernardi et al. and the HRTEM observations the DSC results are attributed to a CNT-mediated entropic effect: due to their intrinsic, 1D cylindrical shape the CNT impose an increased conjugation length on chains adsorbed and stacked upon dispersed CNT. Crystallization thus commences from a heterogeneous mixture of native chains and chains with a longer persistence length (higher effective rigidity) and consequentially a lower effective height of the entropic barrier for crystallization. The findings offer a new insight into the origins of CNT-induced polymer nucleation.

© 2013 Elsevier Ltd. All rights reserved.

1. Introduction

Crystallization from the melt of a synthetic polymer may be viewed as an ordering transition where a collection of random Gaussian chains is transformed into an ordered array of well stacked segments. The consequential loss of conformational entropy of the polymer chains is balanced by the gain in enthalpy [1]. The importance of pre-ordering of the polymer chains in the melt phase for the onset of crystallization is a highly debated topic [2]. Ordering may take place on the molecular level and as a result an increase in the persistence length of the chains will be observed or on a mesoscopic level where liquid-crystalline like phases would be detected [3–5].

Conjugated polymers such as Poly(3-alkyl thiophenes), P3ATs, and specifically regioregular [6] poly-3-hexylthiophene (rr-P3HT) are a benchmark in organic photovoltaics (OPV) [7,8]. In this field device fabrication is based on solution processing of the components into nanometrically thin films. Both good solubility and a high degree of molecular ordering and crystallinity of the polymers in the dried state are crucial for device performance [9,10]. While

conjugated polymers are often perceived as rigid molecules, solvated P3ATs were found to behave as semi-flexible polymers with a persistence length (which is directly related to the conjugation length) [11] below 3 nm in good solvents [12–14]. Yet polymer crystallization, either from the solution or the melt, requires stretched backbone conformations with conjugation length of 20–25 monomers [15,16].

Furthermore, in devices such as bulk heterojunction organic solar cells [15,17] the photoactive layers are made by blending P3HT (and other conjugated polymers) with high concentrations (>50 wt %) of electron acceptors such as fullerenes or fullerene derivatives and recently also carbon nanotubes (CNT) and graphene [18,19].

The detailed interaction between the carbonaceous nanostructures and P3ATs in solution and in the melt is not yet well understood [20–23]. While fullerenes and fullerene derivatives ([6,6]-Phenyl C₆₁ butyric acid methyl ester (PCBM)) were shown to disrupt the crystallization of P3HT and Poly(3-octylthiophene-2,5-diyl) P3OT, CNT and graphene are expected to enhance the degree of crystallinity of the semi-crystalline P3ATs [24,25] probably due to induced nucleation.

Here we describe a detailed investigation of the effect of CNT, PCBM and graphene on the non-isothermal crystallization from the melt of P3HT and P3OT. We use commercially available, highly soluble P3HT and P3OT with designated regioregularity of ~90%

* Corresponding author. Tel.: +972 8 6461272.

E-mail address: rachely@bgu.ac.il (R. Yerushalmi-Rozen).

Table 1
As received powders of carbon nanotubes synthesized via catalytic CVD.

Sample	Diameter (nm) and length (μm)	Purity (vol)	Manufacturer
SWNT-Nanoledge	$d \sim 1\text{--}2$ $l \sim 2\text{--}3$	>90%	Nanoledge S.A France http://www.nanoledge.com/
MWNT-Arkema	$d \sim 10\text{--}15$ $l \sim 10$	\(\sim 85\%	Arkema, France http://www.arkema.com/
MWNT-MER	$d \sim 35 \pm 10$ $l \sim 30$	>90%	MER corporation, Tucson, AZ USA http://mercorp.com/nano.pdf

and 90–95% respectively, and intermediate molecular weight (<80,000 gr/mol) which exhibit a relatively low degree of crystallinity in their native state. The carbonaceous nano-structures are dispersed in the polymer solutions, the dispersions are dried, and their non-isothermal crystallization is monitored via Differential Scanning Calorimetry (DSC). A significant increase in polymer crystallinity as compared to that of the native polymers is only observed in the presence of CNT, while PCBM reduce the degree of crystallinity of the native polymers and a high concentration of graphene (20 wt%) does not affect it. The effect of the CNT strongly depends on their geometry and diameter: at concentration of 25 wt % Multi-Walled Carbon nanotubes (MWNT) increase the degree of crystallinity from about 40% of the native P3HT to \(\sim 62\%\) in the blend. Similar results are obtained for P3OT, a more soluble P3AT derivative: here 25 wt% of MWNT results in crystallinity of 68%. The thermograms reveal a reduction in the degree of under-cooling and the appearance of a double crystallization peak which to the best of our knowledge was not reported before for this system. The two features are only observed following a dispersion procedure which results in elongation and stretching of chains adsorbed at the CNT surface in the solution, as indicated by high resolution transmission electron microscopy (HRTEM) of the dried dispersions. Similar behavior is *not observed* following solvent-mixing which does not lead to polymer adsorption onto the CNT. P3HT and P3OT show a double-crystallization peak and a shift in the crystallization and melting temperatures also in the presence of Single wall carbon nanotubes (SWNT) which are most efficient at a concentration of around 10 wt% where a maximum in the degree of crystallinity (for P3HT, 54%) is obtained.

We rationalize the effect of CNT on the crystallization processes following a detailed molecular study by Bernardi et al. [22] and suggest that the intrinsic, 1D cylindrical geometry of the CNT modifies the conformational state of both the adsorbed polymer chains, and chains stacked upon them, leading to a longer conjugation length as compared to solvated chains. This conformational change is carried out into the melt state where native and CNT-templated chains are distinguished by their effective rigidity and thus the height of the entropic barrier for their crystallization [1]. This behavior is very different from the thermal behavior of fullerenes in PCBM-P3HT composites and graphene, prepared using the very same procedure: both exhibit a single crystallization peak, and the PCBM composites also show an increased degree of undercooling and a lower degree of crystallinity in accordance with previous reports [15,17].

2. Experimental

2.1. Materials

Poly(3-hexylthiophene-2,5-diyl), P3HT, (catalog no.P100, batch BS19-74), regioregularity 90%, Mw = 58,000 gr/mol and Pd = 2.2 and Poly(3-octylthiophene-2,5-diyl), P3OT, (catalog no. 4003-e,

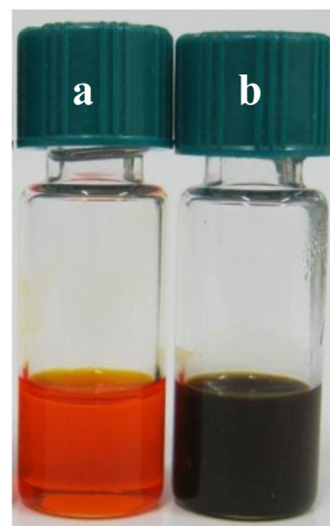
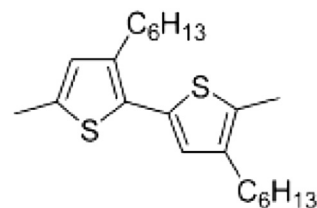


Fig. 1. (a) 5 wt% P3HT in chloroform (b) dispersion of 35 wt% MWNT-MER in P3HT (chloroform).

batch BS16-59) regioregularity \(\sim 90\%\)–95%, Mw = 71,000 gr/mol and Pd = 2.1 were purchased from Rieke Metals. Chloroform (spectroscopic grade) was purchased from Sigma–Aldrich, [6,6]-Phenyl C₆₁ butyric acid methyl ester (PCBM), was purchased from American Dye Source, catalog no. ADS61BFB, purity of >99%.

Graphene nanoplatelets (neat, highly crystalline, Grade 4, Research Grade >700 m²/g, <4 layers) was purchased from cheaptubes (<http://cheaptubes.com>).

The characteristics of the Carbon Nanotubes powders are given in Table 1.

2.2. Sample preparation

2.2.1. Preparation of polymer solutions

Solutions were prepared by dissolving the polymer (P3HT or P3OT) in chloroform and mixing for 24 h.

2.2.2. Preparation of dispersions

Typically 1 ml of dispersion was prepared by adding 2 mg of a dry powder of as- received CNT or graphene to a chloroform solution of the polymer, at the required concentration. The mixture was sonicated (50 W, 43 KHz) for 1 h. The resulting dispersion was centrifuged (20 min at 4500 rpm). Following centrifugation the supernatant was decanted from above the sediment and further used (Fig. 1a, b) [26]. The CNT-to-polymer ratios reported throughout the study are the initial values, introducing an error of less than 0.5 wt%.

The minimal polymer concentration necessary for the formation of stable dispersions of individual SWNT, MWNT or graphene (designated the threshold concentrations C_T) was determined for each of the CNT samples and polymers (P3HT and P3OT). At this concentration the dispersion is stable and agglomeration does not take place following centrifugation and prolonged incubation. Typical values of C_T were found to be in the range of 0.01–0.1

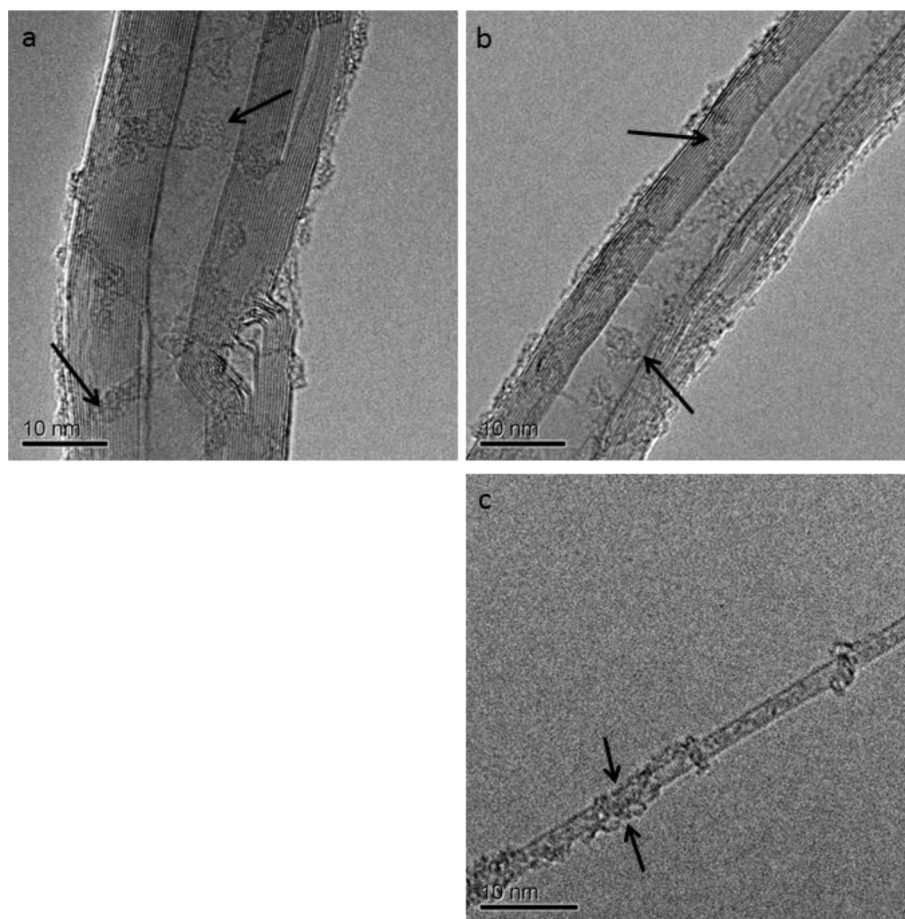


Fig. 2. HRTEM images of samples prepared by drying chloroform dispersions of CNT at the threshold concentration for dispersion C_T (see the [Methods Section](#)). (a) MWNT-MER dispersed by P3HT (b) MWNT-Arkema dispersed by P3OT (c) SWNT-Nanoleedge dispersed by P3HT. The arrows point to polymer segments wrapped around the CNT. The interlayer distance in the MWNT is in agreement with previously reported values (0.34–0.39 nm) [27].

polymer wt% depending on the type of CNT and the dispersing polymer. Dispersions with higher polymer concentrations were prepared by addition of the required polymer amount to a stable CNT-polymer dispersion in chloroform.

The microscopic structure of the dispersions was examined using HRTEM (FEI Tecnai 12 G² TWIN TEM equipped with a Gatan model 794 CCD camera at 120 kV). The specimens were prepared by placing a droplet of the dispersion on a TEM grid (300 mesh Cu, Ted Pella) and drying.

2.2.3. Preparation of samples for DSC measurements

CNT and graphene-polymer blends at different ratios were prepared by drying dispersions prepared as described above for ~2 h at ~45 °C in a fumehood followed by annealing in a vacuum oven at 35 °C for 24 h. Thermal Gravimetric Analysis (TGA, SDTA851, Mettler Toledo) with dry nitrogen (99.999 purity) as purge gas (30 ml min⁻¹) was used to verify that the samples are completely dry and free of solvent leftovers. 9–11 mg of the dry powders were loaded into sealed aluminum crucibles (40 μ l) and measured following the procedure described below. Similar procedure was used for the preparation of the native polymer samples.

2.3. Methods

Differential Scanning Calorimetry (DSC) which is a thermo-analytical technique that records heat flux changes as a function of time served as the main experimental tool in this study (DSC 823e

(Thermal Analysis-METTLER TOLEDO)). Dry nitrogen (99.999 purity) was used as the purge gas (80 ml min⁻¹) and air as a cooling gas. Temperature and enthalpy calibration was carried out using Indium (Mettler). In the “standard” procedure the sample was heated from 30 °C to 260 °C and cooled back at a constant rate, β ($\beta = dT/dt$) = ± 10 °C min⁻¹, where T is temperature and t is time. Between the heating and the cooling cycles the sample was maintained for 45 min at 260 °C and for 10 min at 30 °C. All measurements were repeated 3 times, showing a high degree of reproducibility between the 2nd and 3rd scans (data from the 1st scan is not reported).

Thermograms of the native P3HT measured via the standard heating-cooling sequence described above were used as a reference system. The melting enthalpy per gram of the polymer was calculated from the area enclosed between the heating curve and the baseline (red dotted line, [Fig. S1 Supplementary Data](#)).

The measured and calculated thermal parameters are listed in [Table S1 \(and for P3OT in Table S4 in the Supplementary Data\)](#). These include the degree of super-cooling $\Delta T = T_m - T_{CNT}$ and the percent of crystallinity %C which is calculated from the measured melting enthalpy according to the relation $\%C = [\Delta H / \Delta H_0(1 - \phi)] \times 100$ using the recently suggested value for a fully crystalline P3HT²⁶ $\Delta H_0 = 37$ Jgr⁻¹ and a calculated value for P3OT, $\Delta H_0 = 28$ Jgr⁻¹.

3. Results and discussion

Polymer assembly from chloroform solution onto dispersed CNT was probed using HRTEM imaging. In [Fig. 2\(a\)–\(c\)](#) we present

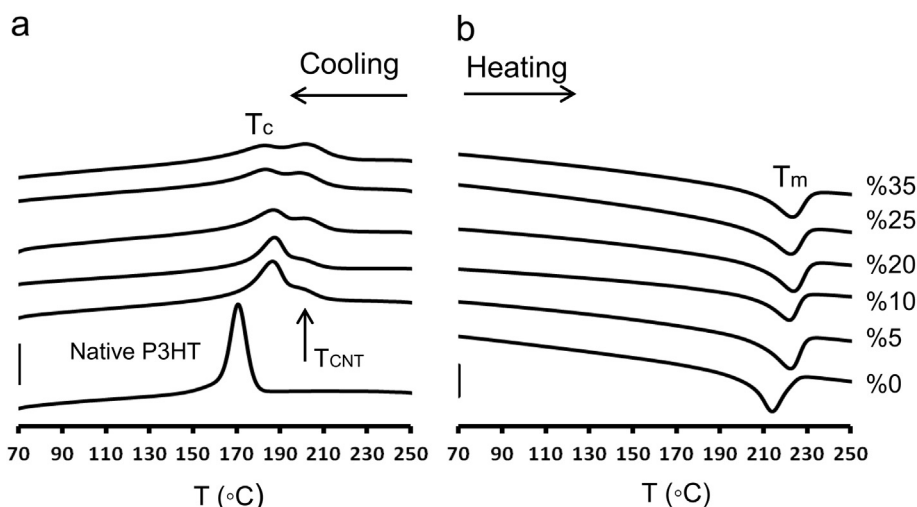


Fig. 3. DSC thermograms of MWNT-MER P3HT composites with different relative weight percent of the MWNT. (a) Cooling (b) heating. T_{CNT} is the exothermic peak observed in cooling blends that contain CNT. The bar indicates 1 mW.

HRTEM images of dried samples taken from P3HT dispersions of MWNT-MER and SWNT-Nanoledge, and P3OT dispersions of MWNT-Arkema (prepared as described in the [Experimental Section](#)) [26]. In these images we clearly see strands of P3HT chains stacked upon MWNT ([Fig. 2\(a\),\(b\)](#)) and coiled around SWNT ([Fig. 1\(c\)](#)) in an irregular manner. Polymer coiling around the narrow (2 nm diameter) SWNT is consistent with the high flexibility of the polymer in good solvent conditions. The images are taken from dispersions at low polymer concentrations so as to expose the pre-crystallization assembly of polymers at the CNT surface. The observed chain configurations are consistent with a recent study by Bernardi et al. [22] where a combination of molecular dynamic simulations and optical absorption measurements demonstrated that the CNT template planar chain conformations of adsorbed chains leading to a significant increase of the conjugation length as compared to solvated chains. In particular, Bernardi et al. report that 20 vol% dispersion of 15 nm long SWNT increased the conjugation length from 4 monomers to 10 monomers (about 4 nm) [22]. The study suggests that the effect on chain conformations results from the intrinsic cylindrical, one dimensional geometry of the tubes and their high aspect ratio. We note here that the CNT used in our study are 2 orders of magnitudes longer than the simulated tubes.

Similar dispersions of MWNT or SWNT in chloroform solutions of P3HT or P3OT, at different polymer-CNT ratios were dried and used for investigation of the thermal behavior of the resulting blends using DSC. The CNT varied in their diameter; 1–2 nm (SWNT-Nanoledge), 10–15 nm (MWNT-Arkema) and 25–35 nm (MWNT-MER) ([Table 1](#)) but were of similar averages lengths (2–30 μm).

In [Fig. 3](#) cooling ([Fig. 3\(a\)](#)) and heating curves ([Fig. 3\(b\)](#)) of P3HT + MWNT-MER composites at MWNT concentrations ranging from 0 wt% to 35 wt % are presented.

The thermograms show a new thermal transition in the cooling curve of the composites ([Fig. 3\(a\)](#), T_{CNT}) at a temperature higher than the crystallization temperature of the native P3HT. This new thermal event appears as a leg at the lowest MWNT-MER concentrations ([Fig. 3\(a\)](#) 5 wt% and 10 wt% MWNT-MER) and develops into a new peak, T_{CNT} , as the concentration of the MWNT increases. The peak temperature does not vary with the MWNT concentration. The temperature of the second peak, designated T_c , is higher than that observed in the native polymer ~ 186 $^{\circ}\text{C}$, and does not change significantly with the concentration of the CNT. The area of the peak located at T_{CNT} (and the calculated crystallization enthalpy) increases, while the area of that observed at T_c decreases. Overall, as the concentration of the MWNT-MER in the blend increases a larger fraction of the polymer crystallizes: The degree of crystallinity as calculated from the normalized enthalpy of the melting peak increases from 40% in the pristine P3HT to 59% ([Table 2](#), %C) in a composite containing 35 wt% MWNT-MER.

In addition, it is found that the melting temperature T_m ([Fig. 3\(b\)](#)) increases by 8 $^{\circ}\text{C}$ indicating a higher stability of the formed crystals. The numerical values are presented in [Table 2](#). The combined effect is a significant decrease in the degree of under-cooling as a function of the concentration of MWNT-MER.

Thermograms of composites comprising P3HT-MWNT-Arkema, P3HT-SWNT-Nanoledge, P3OT-MWNT and P3OT-SWNT show a qualitatively similar behavior: A new thermal transition appears, the enthalpy of the transition increases with the weight percent of the SWNT in the composite, and the melting temperature is shifted to higher values ([Fig. S2–S6](#) and [Tables S2–S6](#) in the [Supplementary Data](#)). The degree of crystallinity is found to increase, reaching a value of 62% at a concentration of 25 wt% MWNT-MER in P3HT, and a value of 68% in a P3OT-CNT blend that contains 25 wt% of MWNT-MER.

Table 2

Thermal parameters obtained from non-isothermal crystallization exotherms and melting endotherms of P3HT- MWNT-MER composites.

	P3HT	5% MWNT-MER	10% MWNT-MER	20% MWNT-MER	25% MWNT-MER	35% MWNT-MER
T_c ($^{\circ}\text{C}$)	170	186	187	186	183	184
T_{CNT} ($^{\circ}\text{C}$)	–	–	–	203	202	201
T_m ($^{\circ}\text{C}$)	214	222	222	223	222	223
ΔH_m (J g^{-1})	15	18	19	20	20	22
$T_m - T_c$ ($^{\circ}\text{C}$)	44	36	35	20	20	22
%C	40	49	51	54	54	59

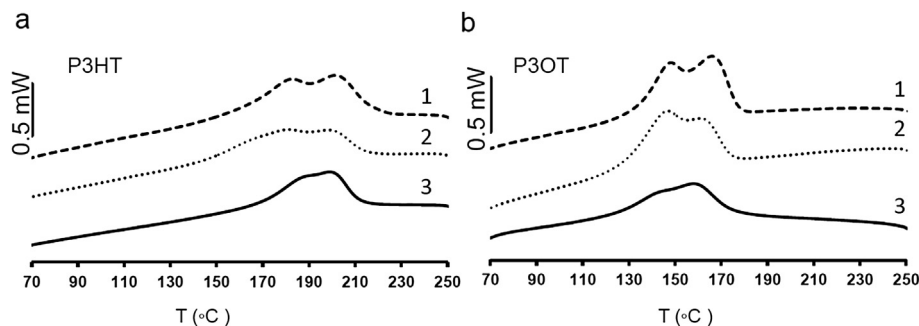


Fig. 4. DSC thermograms presenting the cooling sequence measured in composites containing 35 wt% of CNT (a) in P3HT (b) in P3OT. 1) SWNT-Nanoledge 2) MWNT-Arkema 3) MWNT-MER.

While the detailed thermal behavior of the different polymer – CNT composites is not identical (see below) two common findings stand out: the appearance of double-crystallization peaks, and the significant increase in the degree of crystallinity of the conjugated polymers (P3HT and P3OT). The two (overlapping) thermal peaks which designate the occurrence of two thermal transitions are clearly observed in Fig. 4(a) where cooling curves of composites containing 35 wt% of the three different types of CNT are presented. It seems that the peaks are more resolved in the case of the MWNT of the higher diameter (MWNT-MER). A similar behavior is observed for blends of P3OT (Fig. 4(b)).

We suggest that the multiple crystallization peaks result from the existence of two (or more) populations of chains; native and CNT-templated chains, distinguished by their conformational entropy and consequentially the effective height of the entropic barrier for crystallization of the chains. Upon cooling of the molten blend, crystallization of each of these populations is initiated from a

different conformational state. In this picture the higher crystallization temperature is that of the more rigid chains, due to the lower entropic penalty on their crystallization [28].

In Fig. 5 we present the overall degree of crystallinity (as calculated from the melting enthalpy) and the melting temperature (right axis) as a function of CNT concentrations for P3HT (Fig. 5(a)) and P3OT (Fig. 5(b)). Similar qualitative behavior is observed for the different types of CNT: As CNT-induced crystallization takes place at a higher temperature than that of the native polymers, a higher fraction of the melt is able to crystallize when the cooling is carried at a given rate.

We note here that the absolute degree of crystallinity is calculated using a value recently reported by Pascui et al. [25]. While the actual reference value for 100% crystalline P3HT may be debated, a significant increase in the relative degree of crystallinity of both P3HT and P3OT is clearly observed in our study. We also note that the crystallinity reported here for CNT-induced crystallization is somewhat

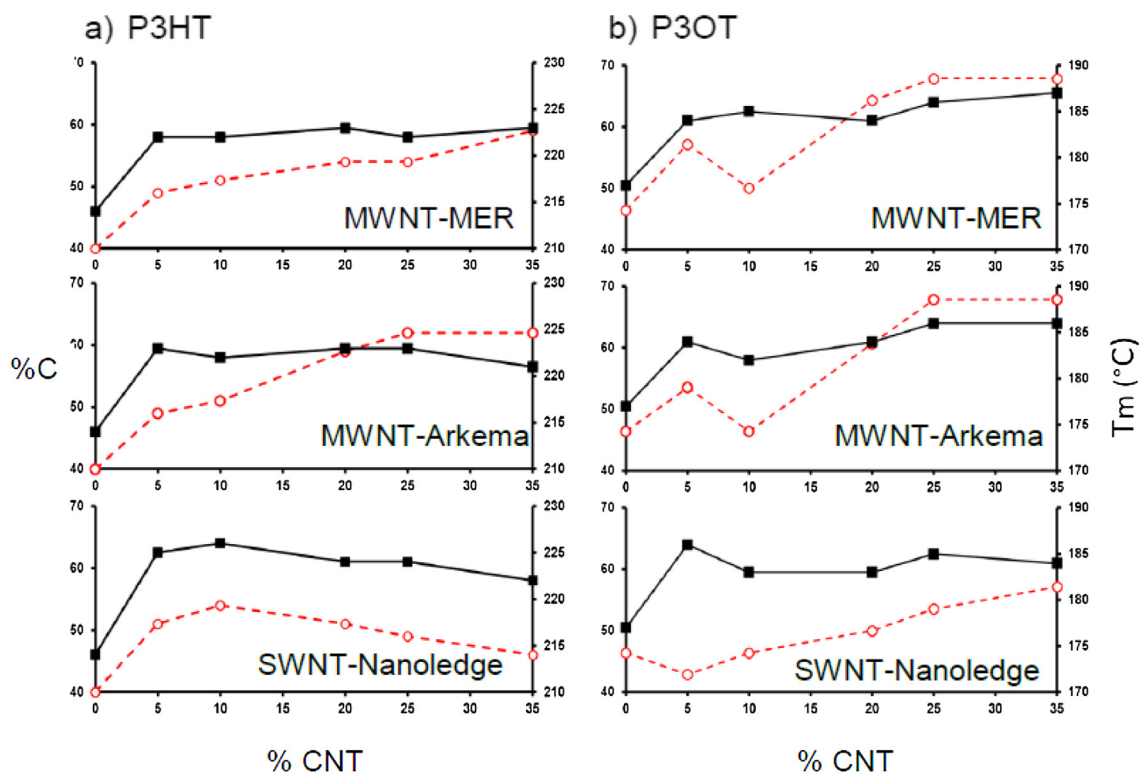


Fig. 5. The degree of crystallization (left) calculated following Ref. [27] and melting temperature (right) obtained from the DSC thermograms in composites of (a) P3HT (b) P3OT as a function of CNT concentrations. The red (dotted) curves are the degree of crystallinity and the black curve is the melting temperature. (For interpretation of the references to color in this figure legend, the reader is referred to the web version of this article.)

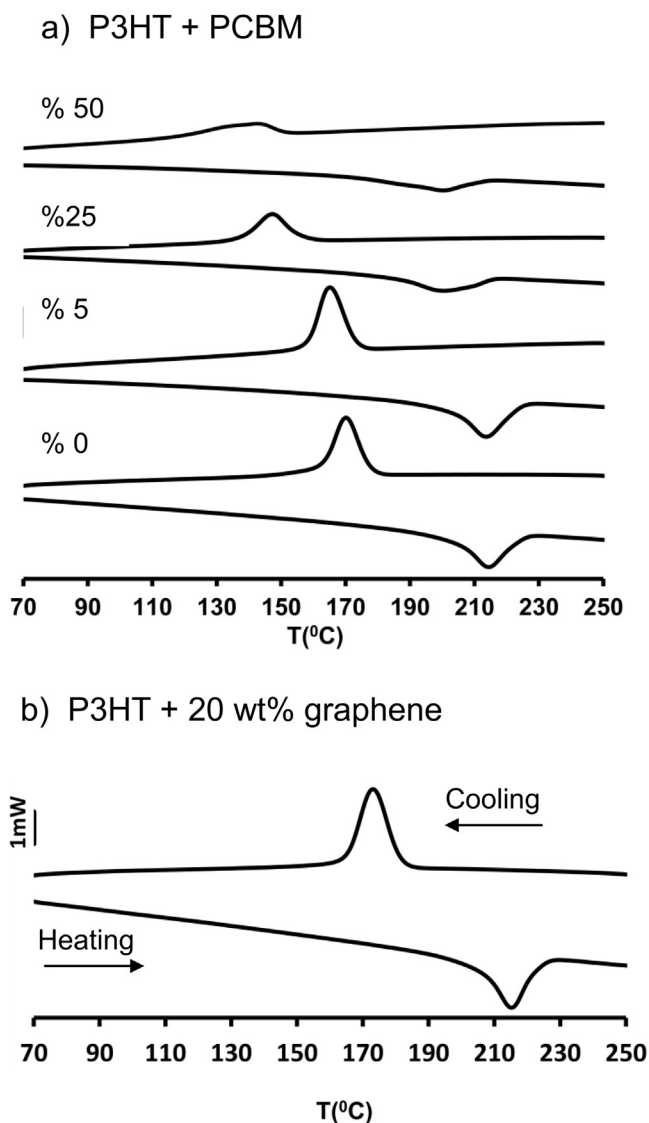


Fig. 6. DSC thermograms of P3HT composites with (a) different concentrations of PCBM from 0 wt% (native P3HT) to 50 wt% PCBM (The thermal data is presented in Table S7) (b) 20 wt% graphene.

lower than the 70% crystallinity (calculated using the same reference value of Ref. [25]) recently reported for defect free meticulously designed and synthesized rr-P3HT [16], it presents a significant improvement over the degree of crystallinity of the native materials.

Analysis of the melting behavior provides additional insight into the effect of the CNT on the thermal behavior of the system: The equilibrium melting temperature T_m^0 , is determined by the condition of equal chemical potential per repeat unit in the melt and crystalline phase, and thus $T_m^0 = \Delta h / \Delta s$ where Δh is the latent heat of melting (fusion) and Δs is the entropy of fusion (both per segment) [1,28,29]. As we assume that crystallization and melting do not disrupt the CNT-polymer complex but rather affect their organization within the melt, the enthalpy of the transition should be similar for adsorbed and free chains, while the entropic gain due to melting would be smaller for the population of polymer chains which were forced into a rigid conformation by the CNT, as they do not gain as much conformational entropy from the transition between the crystal and the melt as do the free chains. Following the rationale presented above, the melting temperature is expected, and observed, to rise in the composites. One should note that we

observe a double crystallization peak, but only a single melting peak. This observation is consistent with a crystallization scenario in which preliminary nucleation at the CNT surface by stretched chains is followed by secondary nucleation on top leading to the formation of a single population of crystals.

The scenario described above is also consistent with the observations that MWNT are more efficient than SWNT in templating the crystallization of the polymers. Indeed, following the HRTEM images (Fig. 2(a),(b)) where chains stacked upon the MWNT are shown to present a much more extended configuration than that of the chains coiled onto the narrower SWNT (Fig. 2(c)), they should impose a higher entropic constraint. This in turn should lead to a lower entropic barrier on crystallization and in the type of experiments presented here, a diameter-dependent crystallization-and-melting behavior, as indeed observed (Fig. 5).

The non-isothermal crystallization of P3HT-PCBM composites at concentration range of 0–50 wt% and 20 wt% graphene was investigated following a similar procedure. The thermograms and the thermal data are presented in Fig. 6 (and Table S7 of the Supplementary Data). In accordance with previous studies [30,31] the presence of the PCBM is found to perturb the crystallization of the polymer, and reduce the degree of crystallinity as compared to the native P3HT. We also observe that a significant fraction of graphene does not affect the crystallization.

The role of conformational selection in polymer crystallization has been recognized in the Hoffman–Lauritzen model [32,33] where nucleation is the rate-determining step, and in the model suggested by Sadler [34] which describes the growth process of polymeric crystals as a sequence of conformational transformations and selection. A conceptually different model developed many years later by Strobl and coworkers [2,35], suggests that polymer crystallization from the melt may evolve by cooperative ordering over large regions. The latter concept resulted in a proliferation of studies where the presence of a liquid phase of different density and a modified conformational state of the chains was inferred [36]. These studies suggest that on the molecular scale the transient pre-crystalline state involves chains stiffening and an increased persistence length and in some cases the formation of an oriented liquid phase. It is thus expected that crystallization from the melt of conjugated polymers would be accelerated and consequentially the degree of crystallization in semi-crystalline materials enhanced, by the presence of chains which exhibit a longer conjugations length, whether they lower the barrier for primary nucleation or encourage the formation of a transient phase of more-rigid chains.

While a long ranged templating effect was observed by us in a different system [37] it is yet to be investigated in the system reported here. Our attempts to estimate the ratios of the two populations via optical absorption measurements (Supplementary Data Fig. S8) do not provide significant information. We suggest that methods such as spin-probe ESR [38] would be able to provide molecular information about the conformational state of chains which are not in direct contact with the CNT in P3AT- organic solvent dispersions.

Our findings suggest that P3HT and P3OT reach a similar (high) degree of crystallinity when the composite is prepared from dispersions of CNT. It is often observed that P3OT and other P3AT derivatives with even longer side-chains that induce a higher flexibility and better solubility of the polymers in organic solvents [39], lower the degree of crystallinity of the polymers. However in this study we observe that in the presence of CNT both derivatives show a similar trend of enhanced degree of crystallinity (Figs. 2–4). We note that the calculated degree of crystallinity of P3OT is somewhat higher than that of P3HT, probably due to the combination of the higher regioregularity and molecular weight of the P3OT and the value used for crystallization enthalpy.

4. Conclusions

The mechanism suggested here where conformational bias induced by dispersed CNT on solvated polymer chains enhances the degree of crystallinity from the melt is very different from other entropy dominated mechanisms such as confinement-induced crystallization [40] and shear-flow induced nucleation [41] and offers a new generic tool for engineering the conjugation length of soluble P3AT derivatives in good solvents.

Utilizing the proposed pathway for non-covalent modification of soluble non-regular, commercially available P3AT derivatives so as to enhance their degree of crystallinity in the dried state may offer an alternative for covalent design of highly regular defect free materials. Furthermore, the additives used in this study are expected to enhance the PV efficiency of the active layers prepared from the blends as CNT are known to improve the conductivity of conjugated polymers by offering a pathway for non-hopping conductance of charge carriers.

Acknowledgment

R.Y-R holds the Stanley D. and Nikki Waxberg professorial chair in Advanced Materials. The support of the Israel Science Foundation grant no. 208/09 is acknowledged.

Appendix A. Supplementary data

Supplementary data related to this article can be found at <http://dx.doi.org/10.1016/j.polymer.2013.09.057>.

References

- [1] Rice SA, Muthukumar M. Nucleation in polymer crystallization [Advan Chem Phys]. In: Rice SA, editor. vol. 128; 2004. p. 1–65. Hoboken: New-Jersey, USA.
- [2] Strobl G. A thermodynamic multiphase scheme treating polymer crystallization and melting. *Eur Phys J E* 2005;18:295–309.
- [3] Winokur MJ, Spiegel D, Kim Y, Hotta S, Heeger AJ. Structural and absorption studies of the thermochromic transition in P3HT. *Synth Metals* 1989;28:C419–26.
- [4] Zhao Y, Yuan G, Roche P, Leclerc MA. Calorimetric study of the phase transitions in P3HT. *Polymer* 1995;36:2211–4.
- [5] Hugger S, Thomann R, Heinzl T, Thurn-Albrecht T. Semicrystalline morphology in thin films of P3HT. *Colloid Polym Sci* 2004;282:932–8.
- [6] Regioregularity denotes the percentage of stereoregular head-to-tail (HT) attachments of the hexyl side chains to the 3-position of the thiophene rings.
- [7] Sirringhaus H, Brown PJ, Friend RH, Nielsen MM, Bechgaard K, Langeveld-Voss BMW, et al. *Nature* 1999;401:685.
- [8] Dang MT, Hirsch L, Wantz G. P3HT: PCBM, best seller in polymer photovoltaic research. *Adv Mater* 2011;23:3597–602.
- [9] Lim JA, Liu F, Ferdous S, Muthukumar M, Briseno AL. Polymer semiconductor crystals. *Mater Today* 2010;13:14–24.
- [10] Agostinelli T, Lilliu S, Labram JG, Campoy-Quiles M, Hampton M, Pires E, et al. Real-time investigation of crystallization and phase-segregation dynamics in P3HT: PCBM solar cells during thermal annealing. *Adv Func Mater* 2011;21:1701–8.
- [11] Heffner GW, Pearson DS. Molecular characterization of poly(3-hexylthiophene). *Macromolecules* 1991;24:6295–9.
- [12] Heffner GW, Pearson DS, Gettinger CL. Characterization of poly(3-octylthiophene). I: molecular characterization in dilute solution. *Polym Eng Sci* 1995;35(10):860–7.
- [13] Aime JP, Garrin P. Physical origin of the local rigidity of conjugated polymers in good solvent. *Synth Met* 1991;41:859–67.
- [14] Yang H, JooShin T, Yank L, Cho K, Ryu CY, Bao Z. Effect of mesoscale crystalline structure on the field-effect mobility of RR P3HT in thin film transistor. *Adv Func Mater* 2005;15:671–6.
- [15] Collins BA, Tumbleston JR, Ade H. Miscibility, crystallinity and phase development in P3HT/PCBM solar cells: toward an enlightened understanding of device morphology and stability. *J Phys Chem Lett* 2011;2:3135–45.
- [16] Kohn P, Hüttner S, Komber H, Senkovskyy V, Tkachov R, Kiriya A, et al. On the role of single regiodefects and polydispersity in regioregular poly(3-hexylthiophene): defect distribution, synthesis of defect-free chains, and a simple model for the determination of crystallinity. *J Am Coll Surg* 2012;134:4790–805.
- [17] Lilliu S, Agostinelli T, Pires E, Hampton M, Nelson J, Macdonald JE. Dynamics of crystallization and disorder during annealing of P3HT/PCBM bulk heterojunctions. *Macromolecules* 2011;44:2725–34.
- [18] Li C, Chen Y, Wang Y, Iqbal Z, Chhowalla M, Mitra SJ. A Fullerene-single wall carbon nanotube complex for polymer bulk heterojunction photovoltaic cells. *J Mater.Chem* 2007;17:2406–11.
- [19] Li C, Chen Y, Addo S, Mitra S. Fullerene-multiwalled carbon nanotube complexes for bulk heterojunction photovoltaic cells. *Appl Phys Lett* 2010;96:143303.
- [20] Yang Z, Lu H. Nonisothermal crystallization behaviors of poly(3-hexylthiophene)/reduced graphene oxide nanocomposites. *J Appl Polym Sci* 2013;128:802–10.
- [21] Tuncel D. Non-covalent interactions between carbon nanotubes and conjugated polymers. *Nanoscale* 2011;3:3545–54.
- [22] Bernardi M, Giulianini M, Grossman JC. Self-assembly and its impact on interfacial charge transfer in carbon nanotube/P3HT solar cells. *ACS Nano* 2010;4:6599.
- [23] Geng J, Zeng T. Influence of SWNT induced crystallinity enhancement and morphology change on polymer photovoltaic devices. *J Am Coll Surg* 2006;128:16827–33.
- [24] Derbal-Habak H, Bergeret C, Cousseau J, Nunzi JM. Improving the current density JSC of organic solar cells P3HT: PCBM by structuring the photoactive layer with functionalized SWCNTs. *Sol Energy Mater So Cells* 2011;95:553–6.
- [25] Pascui OF, Lohwasser R, Sommer M, Thelakkat M, Thurn-Albrecht T, Saalwächter K. High crystallinity and nature of crystal-crystal phase transformations in regioregular poly(3-hexylthiophene). *Macromolecules* 2010;43:9401–10.
- [26] Shvartzman-Cohen R, Nativ-Roth E, Baskaran E, Levi-Kalishman Y, Szeifer I, Yerushalmi-Rozen R. Selective dispersion of SWNT in the presence of polymers: the role of molecular and colloidal length scales. *J Am Coll Surg* 2004;126:14850.
- [27] Kiang CH, Endo M, Ajayan PM, Dresselhaus G, Dresselhaus MS. Size effects in carbon nanotubes. *Phys Rev Lett* 1998;81:1869.
- [28] Muthukumar M. Molecular modeling of nucleation in polymers. *Phil Trans R Soc Lond* 2003;A 361:539.
- [29] Mandelkern L. Crystallization of polymers. N.Y: McGraw-Hill; 1964.
- [30] Erb T, Zhokhavets U, Gobsch G, Raleva S, Stühn B, Schilinsky P, et al. Correlation between structural and optical properties of composite polymer/Fullerene films for organic solar cells. *Adv Func Mater* 2005;15:1193–6.
- [31] Vanlaeke P, Swinnen A, Haeldermans I, Vanhoyland G, Aernouts T, Cheyns D, et al. P3HT/PCBM bulk heterojunction solar cells: relation between morphology and electro-optical characteristics. *Solar Energy Mater Solar Cells* 2006;90:215.
- [32] Hoffman JD, Davis GT, Lauritzen JI, Hannay NB. Treatise on solid state chemistry. 3rd ed. N.Y: Plenum Press; 1976. Chap. 7.
- [33] Akcelrud L. Electroluminescent polymers. *Prog Polym Sci* 2003;28:875–962.
- [34] Sadler DM. New explanation for chain folding in polymers. *Nature* 1987;326:174.
- [35] Strobl G. The physics of polymers. 3rd ed. Berlin Germany: Springer –Verlag; 2007.
- [36] Heeley LE, Poh CK, Li W, Maidens A, Bras W, Dolbnya IP, et al. Are metastable, precyrstallisation, density-fluctuations a universal phenomena. *Faraday Discuss* 2003;122:343–61.
- [37] Ben-David O, Nativ-Roth E, Yerushalmi-Rozen R, Gottlieb M. Rheological investigation of single-walled carbon nanotubes – induced structural ordering in CTAB solutions. *Soft Matter* 2009;5:1925–30.
- [38] Shvartzman-Cohen R, Florent M, Goldfarb D, Szeifer I, Yerushalmi-Rozen R. Aggregation and self-assembly of amphiphilic block copolymers in aqueous dispersions of carbon nanotubes. *Langmuir* 2008;24:4625–32.
- [39] Malik S, Nandi A. Crystallization mechanism of regioregular poly(3-alkyl thiophene)s. *J Polym Sci Part B: Polym Phys* 2002;40:2073.
- [40] Alcoutlabi M, McKenna GB. Effects of confinement on material behavior at the nanometre size scale. *J Phys Condens Matter* 2005;17:R461–524.
- [41] Tribout C, Monasse B, Haudin A. Experimental study of shear-induced crystallization of an impact polypropylene copolymer. *Colloid Polym Sci* 1996;274:197–208.